Bichromatic Synthetic Schlieren for surface measurement

Jostein Kolaas[1,*], Lisa Smith[1], Atle Jensen[1], Johan Kristian Sveen[1,2]

1: Dept. of Mathematics, University of Oslo, Norway
2: Institute for Energy Technology, Norway
* Correspondent author: josteiko@math.uio.no

Keywords: Synthetic Schlieren, Background oriented Schlieren, Surface measurements, Solitary wave

ABSTRACT

We introduce Bichromatic Synthetic Schlieren (BiCSS) for instantaneous surface measurements, in where we use two simultaneous images taken at blue and near infrared wavelengths, making use of that refractive index variation depends on wavelength, rather than using a reference/dynamic image pair to measure the surface gradient. Experiments on solitary and periodic waves were used to test the method, showing that new method can produce good results. Using this method it might be possible to extend the wave steepness range of Synthetic Schlieren surface measurements by overcoming the Invertibility Condition caused by light ray crossing, but due to compromises in design of real lenses, it might be difficult to achieve in practice. It might also serve as a first step towards a synthetic Schlieren method without a reference image, making it possible to use these methods in experiments where taking the reference image is difficult or impossible.

1. Introduction

Synthetic Schlieren (Sutherland et al, 1999; Dalziel et al, 2000) or Background Oriented Schlieren (Meier, 2002) is a non-intrusive optical method based on pattern matching often used to measure density/salinity; making use of changing refractive index through a volume. This method can also be used for measuring surface elevation (Moisy et al, 2009). We introduce Bichromatic Synthetic Schlieren (BiCSS) for instantaneous surface measurements, in where we use two simultaneous images taken at blue and near infrared wavelengths, making use of that refractive index variation depends on wavelength, rather than using a reference/dynamic image pair to measure the surface gradient. Absorption of near infrared has also been used for surface measurement, by combining red and near infrared illumination, Jähne (2005) measured wave height by absorption and slope angle using refraction, an extension to his previous work (Jähne, 1990) where the wave slope was determined by refraction using two alternating light source with linear intensity change through a diffusion box instead of a pattern. Aureli et al (2009) further expanded on this concept for use in non-horizontal bottoms. Note that these methods must use light sources with a small difference in wavelengths, as the refraction angle is assumed to be the same for both wavelengths.

2. Method

The general procedure for these types of experiments is to take images using a camera of a fixed pattern through the measurement volume, measure the displacement of the pattern using a pattern matching algorithm and relate this displacement to the surface elevation (or density).
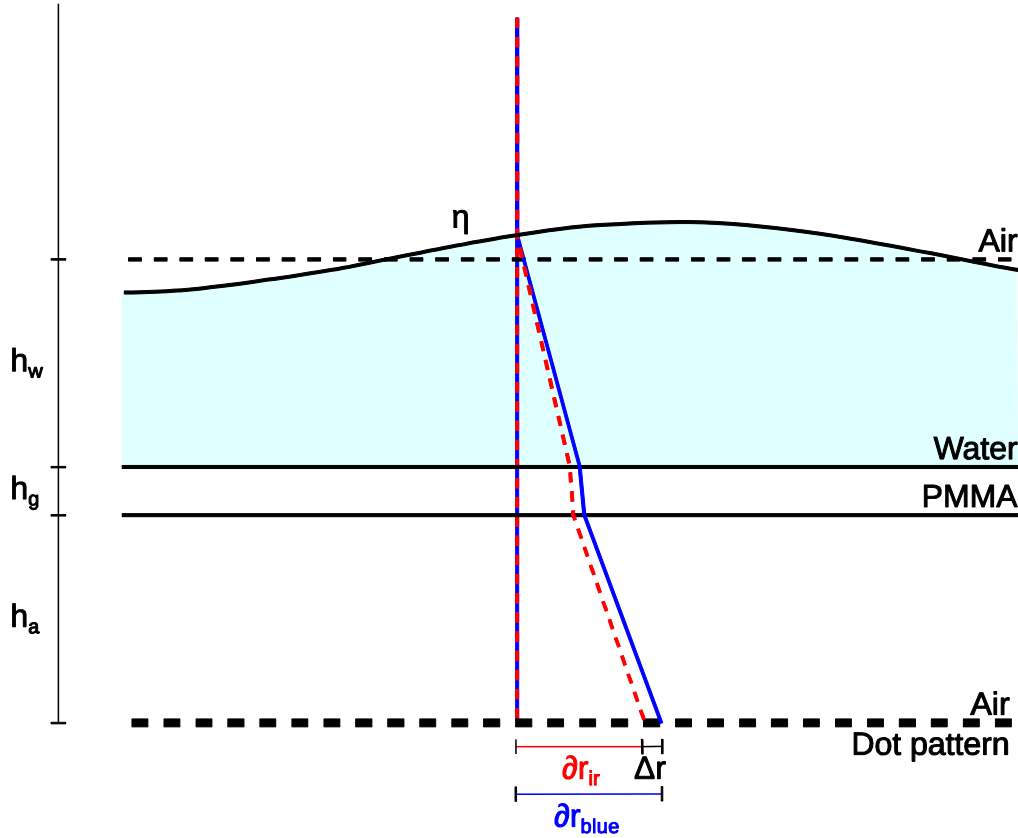

Fig. 1 BiCSS principle

Using the following assumptions

1. *paraxial approximation*: Camera distance, *H*, is much larger than the field of view *L*.
2. *Weak slope approximation*: $|d^2\eta/d^2s| \ll \delta^{-1}$ where δ is a constant dependent on lens aperture.
3. *Weak amplitude approximation*: Apparent distance to pattern, $h_{p,\lambda}$, is much larger then the wave amplitude $|\eta|$.

Moisy et al (2009) showed that the gradient of the surface can be expressed as

$$\nabla h = -\frac{\delta r_\lambda}{h_\lambda^*}, \text{ with } \frac{1}{h_\lambda^*} = \frac{1}{\alpha_\lambda h_{p,\lambda}} - \frac{1}{H} ,$$

(1)

where $\alpha_\lambda = 1 - \frac{n_{a,\lambda}}{n_{w,\lambda}}$, depends on the refractive index of air $n_{a,\lambda}$ and water $n_{w,\lambda}$ and the apparent pattern distance

$$h_{p,\lambda} = h_w + \frac{n_{w,\lambda}}{n_{g,\lambda}} h_g + \frac{n_{w,\lambda}}{n_{a,\lambda}} h_a \,, \tag{2}$$

is adjusted for the Plexiglas thickness h_g and air gap h_a between the wave flume and pattern, where h_w is the water depth. This equation depends on the refractive index which varies with the wavelength, λ. In the present study the refractive indices was estimated using Sellmeier dispersion formula (Sellmeier, 1871)

$$n^2 - 1 = \sum_{i=1}^{4} \frac{A_i \lambda^2}{\lambda^2 - \lambda_i^2} \,, \tag{3}$$

fitted to experimental data from Daimon and Masumura (2007), Ciddor (1996) and Sultanova et al (2009) for water, air and PMMA respectively. Starting with the difference between two wavelength

$$\Delta r = \delta r_{\lambda_{blue}} - \delta r_{\lambda_{ir}} \tag{4}$$

inserting into (1) for each wavelength, λ, and rearranging the terms we get a similar linear equation for the instantaneous surface

$$\nabla h = -\frac{\Delta r}{h^*_{\lambda_{blue},\lambda_{ir}}} \tag{5}$$

with $h^*_{\lambda_{blue},\lambda_{ir}} = h^*_{\lambda_{blue}} - h^*_{\lambda_{ir}}$. Using the difference between two wavelengths puts a stricter requirement on the paraxial approximation, which may require correcting for the displacement when the surface at rest,

$$\nabla h = -\left[\frac{\Delta r}{h^*_{\lambda_{blue},\lambda_{ir}}} - \frac{\Delta r_0}{h^*_{\lambda_{blue},\lambda_{ir}}} \right] \tag{6}$$

In theory a telecentric lens could be used, in which the paraxial approximation is fulfilled per definition. Given that all light rays are perpendicular to the flat surfaces and if there is no chromatic aberration in the lens, there will be no need of a pair of reference images as the

correction term will vanish as $\Delta r_0 \rightarrow \infty$. The coordinate system would also be a fixed property of the CCD size and lens, giving the possibility of a calibration-free measurement system.

Using BiCSS it may be possible to overcome the Invertibility Condition

$$h_{p,\lambda} < \frac{1}{\alpha_\lambda k \eta_0}, \text{ where } \eta = \eta_0 \cos(kx). \tag{7}$$

This shows the maximum pattern distance for a sinusoidal wave to avoid crossing of light rays. This can be seen as a stricter weak slope requirement. Overcoming the Invertibility Condition allows measurements where the depth of the water is larger than the maximum allowed pattern distance $h_w > h_{p,c}$ when using regular free-surface synthetic schlieren. Note that an alternative solution to this problem was been proposed by Gomit et al (2013), involving the use of an extra camera and a light sheet.

2. Experimental setup

The experiments were conducted in 10cm wide and 305cm long wave flume made in PMMA with 6mm wall thickness (h_g), see figure 2. The flume was placed on a traversing table enabling adjustment of the apparent pattern distance $h_{p,\lambda}$ by adjusting the air gap between the flume and pattern. The pattern, a transparent printed using a laser printer, is illuminated using two Advanced illumination BL0404 4"x4" Surface Mount LED Back Light, with peak wavelength 470nm (Blue) and 880nm (NIR). These individual wavelengths are then combined using a cold mirror (reflects visual light, NIR passes through). The LEDs are pulsed at 30Hz with a pulsewidth of 750μs.

To record the pattern deformation a Visual/NIR Camera (jAi AD-130 GE) equipped with a telecentric lens (OPTO Engineering TC12144) was used. The camera separates the visual spectrum from near infrared into 2 CCDs using a hot prism. The visual CCD has a Bayer-filter, so the camera records the image in four channels , red, green, blue and infrared, in which only the blue and infrared channel were used in the experiment. Note that the lens used in this experiment does have some chromatic aberration and is not completely telecentric and thus needs correction for the displacement when the surface is at rest.

To compare the wave elevation a custom made General Acoustics Ultralab ULS Advanced, equipped with ultrasonic wave gauges with a range of 30-250mm.
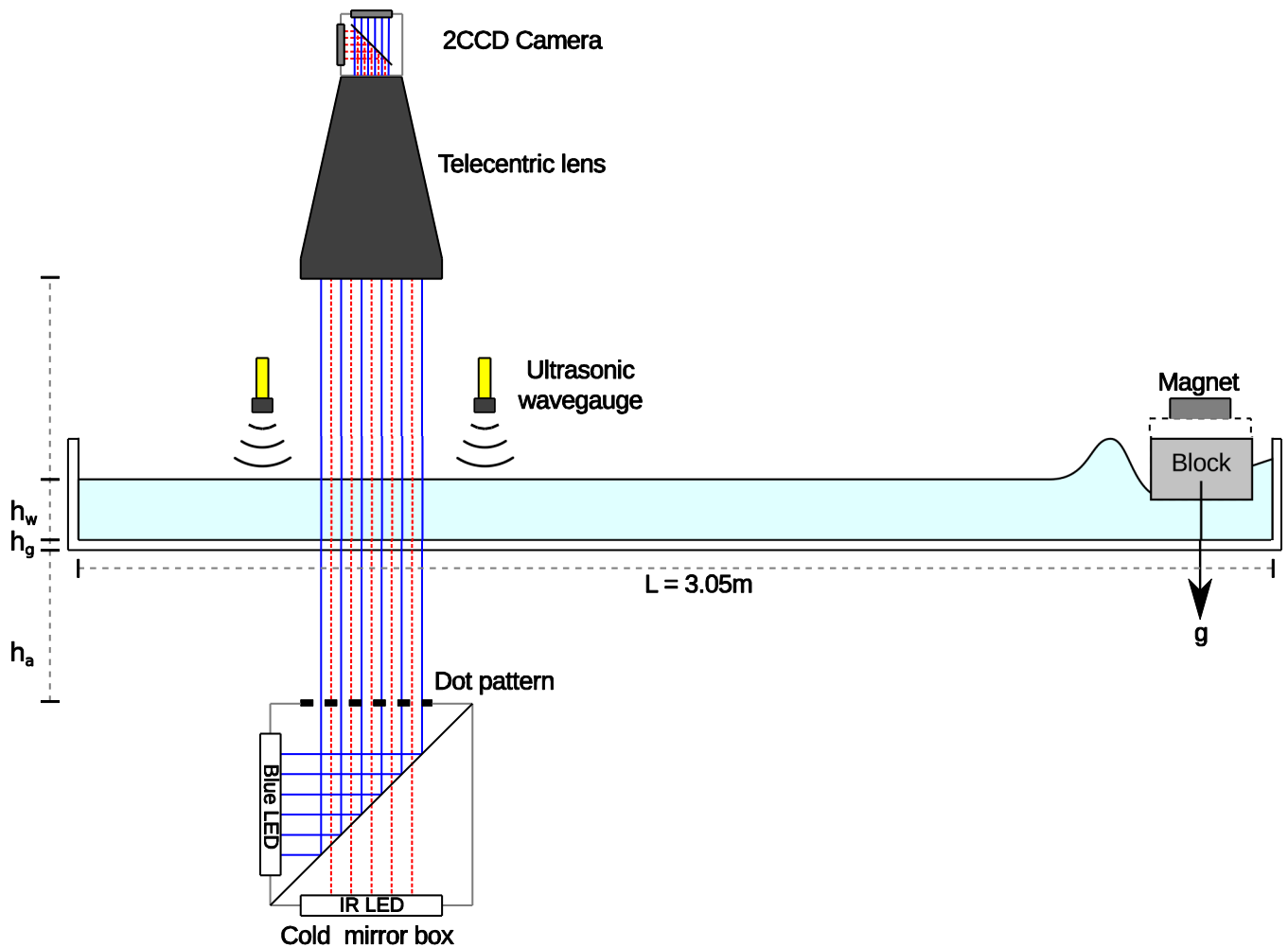
Fig. 2 Experimental setup with Scott-Russel wavemaker

Our in-house particle image velocimetry code, HydrolabPIV (Kolaas, 2016) using multipass with window distortion was used to find the displacement of the pattern and the surface elevation was found by integrating the surface gradient, ∇h, using "Inverse (integrated) gradient" (D'Errico, 2006). For the solitary waves the integration constant was determined by assuming the surface starts at rest.

3. Measurements of solitary waves

Solitary waves were first observed by John Scott Russell in 1834 (Russel, 1844). The waves consisted of one single crest and travel with a constant speed without changing shape. They are nonlinear and dispersive waves. A full potential solution for solitary waves was found by Tanaka (1986), while Fenton (1972) found a ninth order approximate solution for solitary waves. We can use this potential solution with matching wave speed, in addition to the two acoustic wave

probes to compare with the experimental results, see figure 3-5. The solitary wave was generated using a Scott-Russel wavemaker at water depth $h_w = 30$mm.
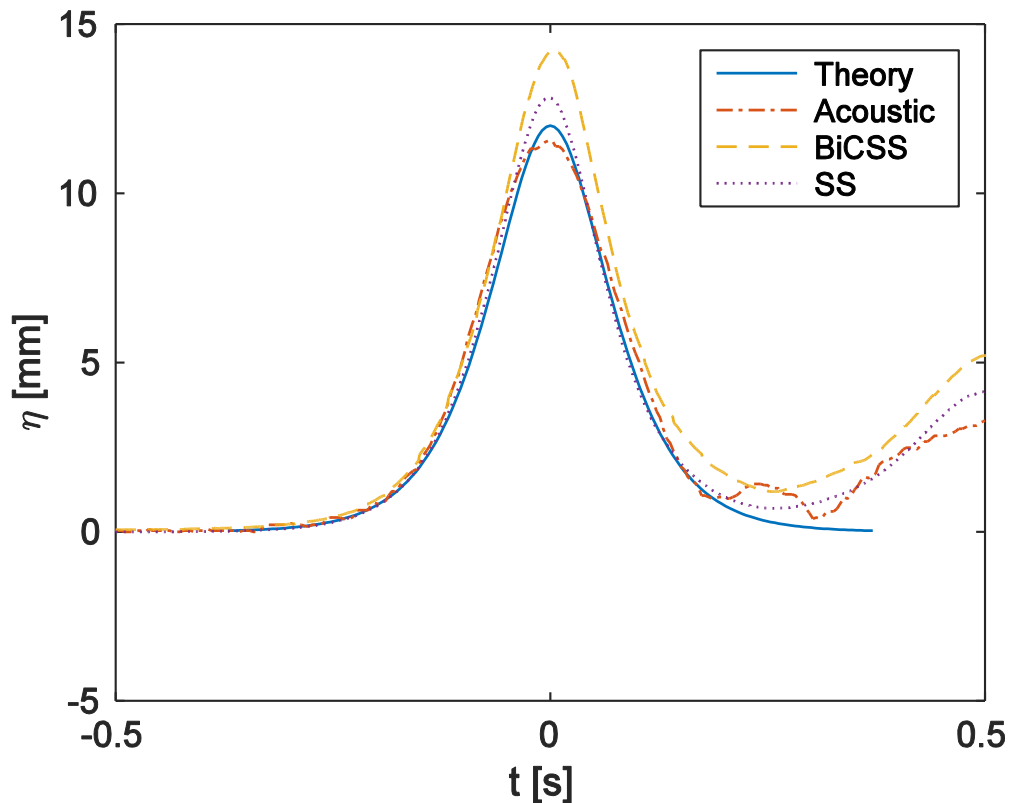

Fig. 3 Surface elevation of solitary wave, $h_a = 2$mm.

Since the wavelength of the solitary wave is much larger than the field of view, we need a method for finding the integration constant. Assuming the wave travels at a constant speed, c, we can use wave the speed found by correlating the acoustic wave probes and correlating with the previous image to find the change in integration constant. The wave speed for the solitary wave was found to be 63.89cm/s. We can compare this with the numerical simulation based on potential theory with dimensionless amplitude $|\eta|/h =0.4$, which gives 63.90cm/s. Also since the camera has limited frame rate, the assumptions that the wave travels at constant speed, $x = ct$ was further used to convert from space x to time t, making use of the spatial resolution, and several time steps stitched together to assemble the complete waveform.
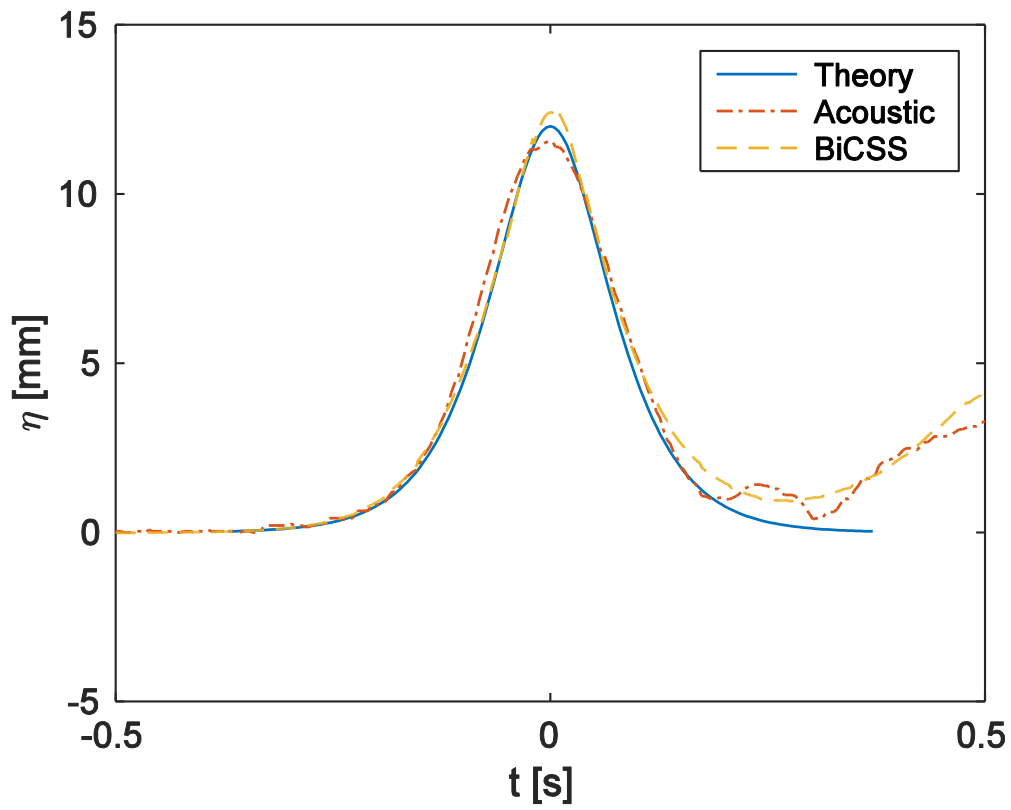
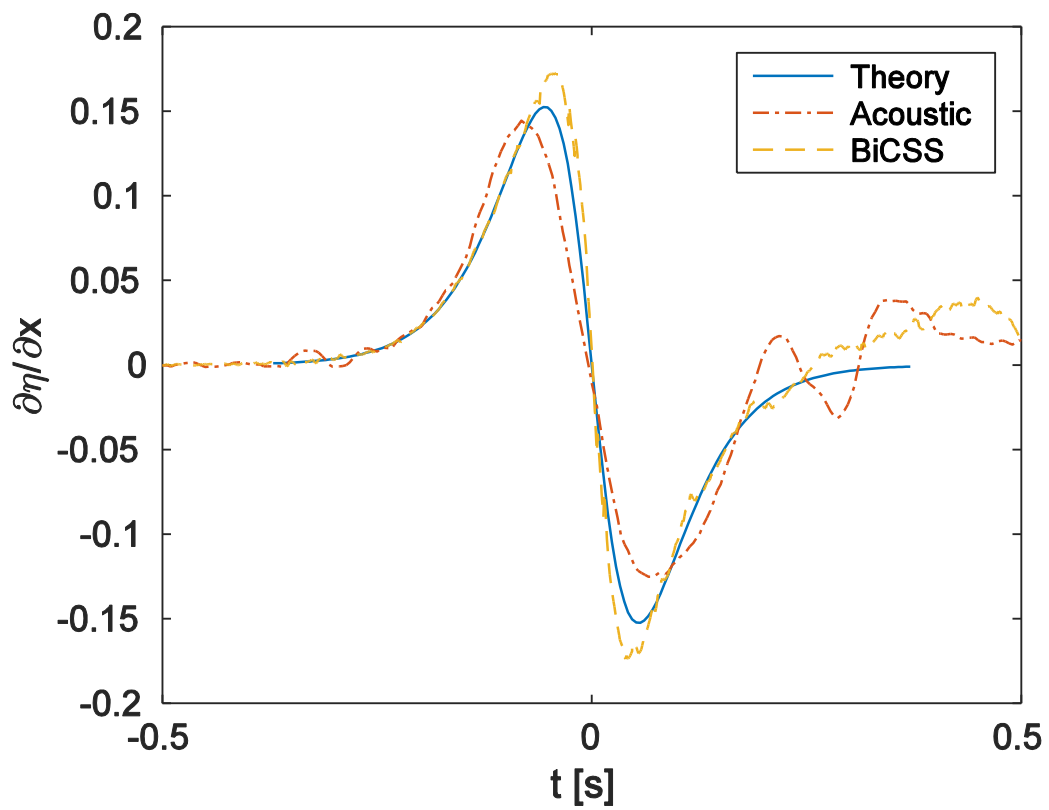**Fig. 4** Surface elevation of solitary wave, $h_a = 50$mm.

Fig. 5 Surface gradient of solitary wave, $h_a = 50$mm.

When the pattern is very close to the flume ($h_a = 2$mm), both Synthetic Schlieren and BiCSS over predicts the surface elevation (BiCSS slightly more), likely due to the weak amplitude approximation. This can be improved by increasing the apparent pattern distance by increasing h_a and we see that BiCSS does indeed give a good match at $h_a = 50$mm. Note that Synthetic Schlieren fails here as the displacements are too large. When looking at the derivative with respect to space BiCSS gives a slightly more acute peak compared to theory, while the acoustic wave probes seem to flatten the peak.

When conducting experiments in wave flumes, secondary waves are induced due to the wall effects. Since BiCSS is a surface measurement method, we have the opportunity to study these waves, which appears cnoidal shape waves traveling at a wave speed 54.23cm/s (approximately linear shallow water speed, $c = \sqrt{gh}$), slightly slower than the solitary wave which traveled at 63.89cm/s. These secondary waves forms crests with 10x10cm and 10x20cm Xs, see figure 6.
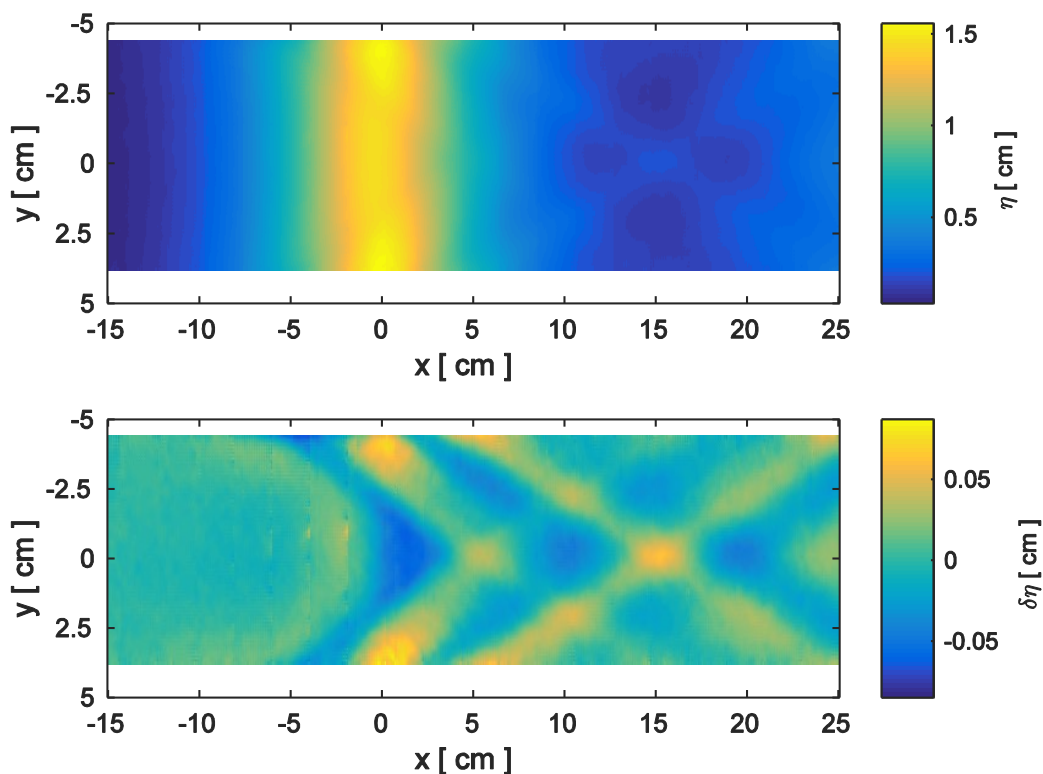

Fig. 6 Surface of solitary wave, the lower plot show the difference from the average over the width of the flume, illustrating secondary effects due to the wall.

4. Periodic waves

To further insight regarding if BiCSS can overcome the Invertibility Condition, a wavemaker for short periodic waves was developed. The wavemaker consist of a 12″ loudspeaker connected to a PMMA-plate with a width of 7.3mm. The plate is located 23cm from the middle of the measurement area, and moves at a rate of 7Hz with an excursion giving a wave height of approximately 1mm at the measurement area. Assuming symmetry the acoustic wave probes was placed on the opposite side of the wavemaker.
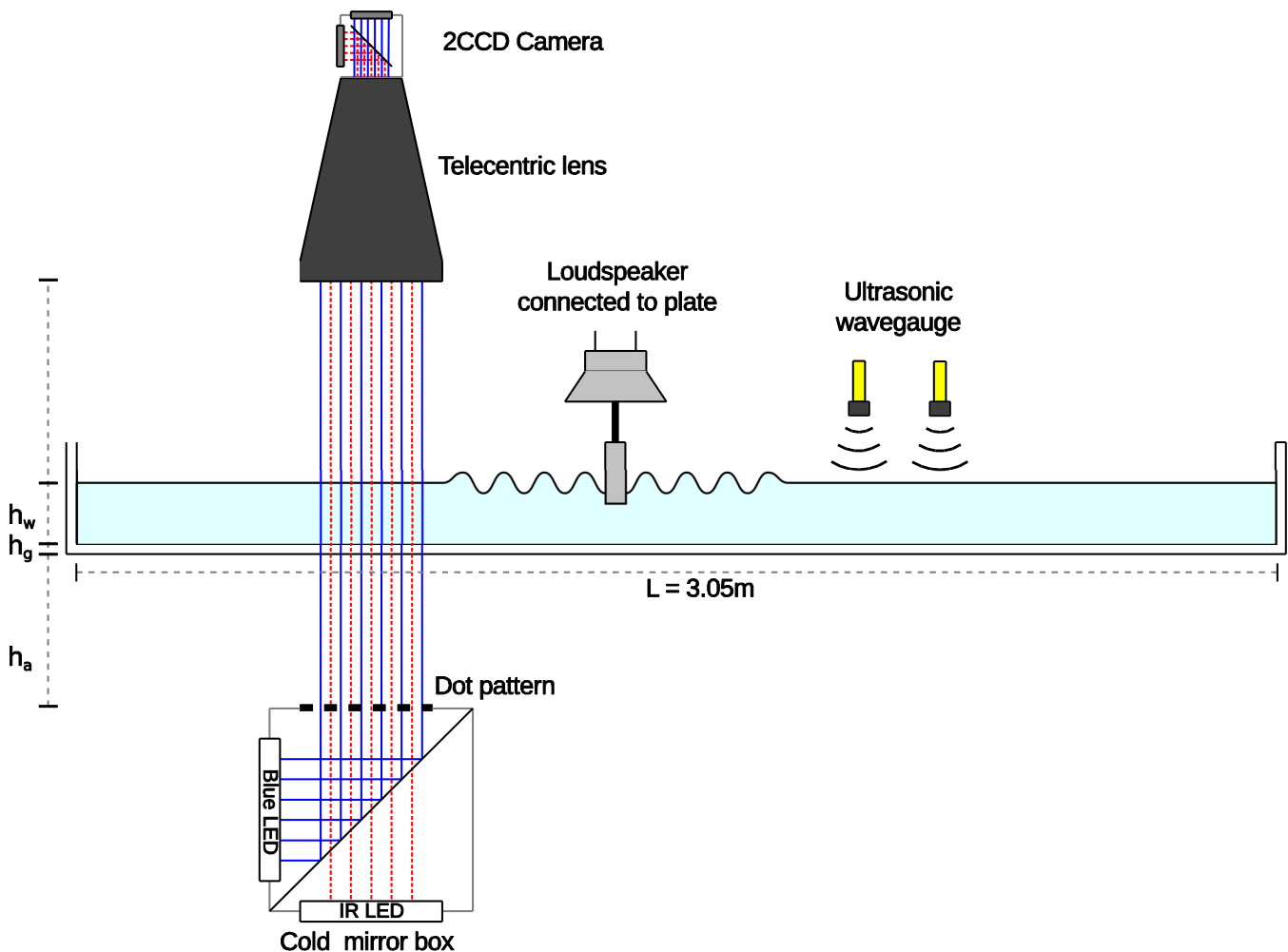
Fig. 7 Experimental setup for periodic waves using loudspeaker based wavemaker.

One can challenge the method as far as possible by increasing the distance between the flume and pattern until the Invertibility Condition does not hold and the light rays crosses as seen in figure 8 at $h_a = 200$mm.

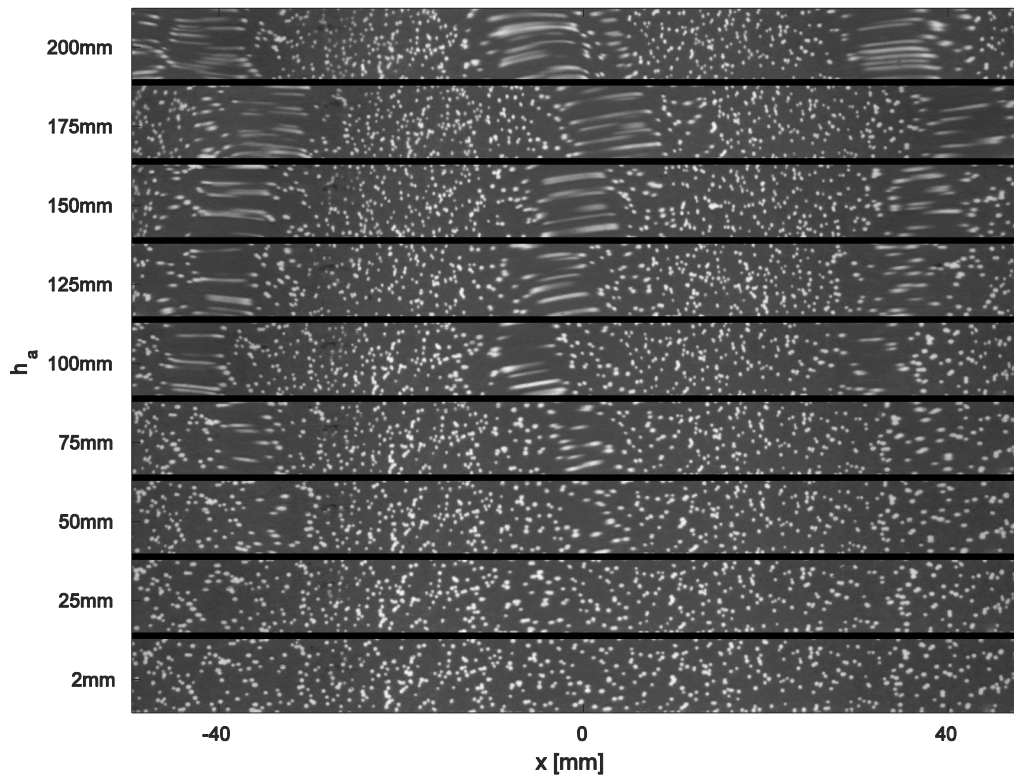**Fig. 8** Surface elevation of solitary wave, $h_a = 50$mm.

While the pattern matching does indeed fail for Synthetic Schlieren when the light ray crosses, it only results in a few wrong vectors, which are easily detected and replaced by a outlier algorithm. The maximum displacement can become huge, varies from 10-80pixels/frame. To accommodate for these large displacement multipass pattern matching algorithm starts with 128x128 pixel subwindow pass and ending with distorted passes with 32x32pixel subwindows. Giving the challenges caused by large distortions of the image, Synthetic Schlieren does remarkably well for all pattern distances.

In comparison, the max displacement for BiCSS is 1.5-15pixel/frame which normally should be much more suitable for the pattern matching algorithm. Even though BiCSS should not be affected by light crossing (there is no crossing in the difference between blue and near infrared), BiCSS does not seem to be an improvement at increased pattern distances. Further investigation into this, involving numerical simulation of the experiment reveals that this is caused by out-of-focus chromatic aberration of the lens, that is the lens used is slightly entocentric at 470nm (Blue), while for 880nm (NIR) it is slightly pericentric. This results in a non-linear interaction between the chromatics behavior of the lens and the chromatic effect of the test section, which increases in strength as pattern distance h_a or wave amplitude increases. Taking these lens

properties into account also predicts the overestimation of BiCSS compared to Synthetic Schlieren seen in the solitary wave measurements.
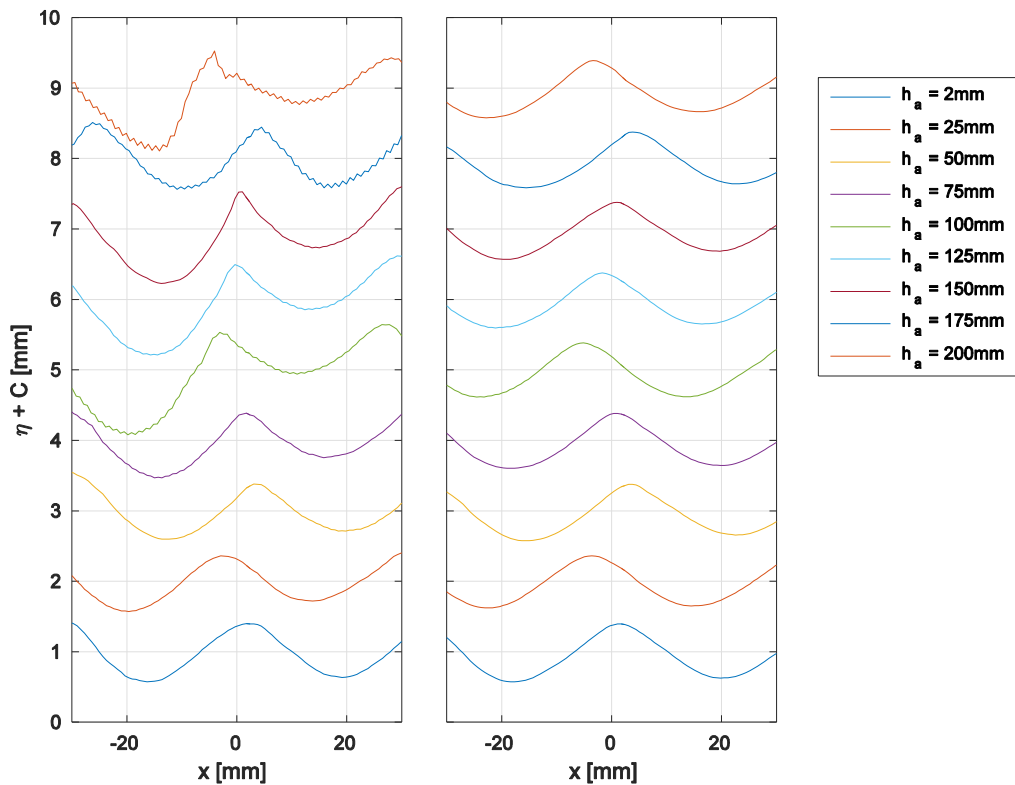

Fig. 9 Surface elevation periodic wave BiCSS (left) and Synthetic Schlieren (right).

5. Conclusions

We have shown that it is possible to use a Synthetic Schlieren type method using two simultaneous images taken at blue and near infrared wavelengths for surface measurements of a solitary wave. Using this method it might be possible to extend the wave steepness range of Synthetic Schlieren surface measurements by overcoming the Invertibility Condition caused by light ray crossing, but due to compromises in design of real lenses, it might be difficult to achieve in practice. It might also serves as a first step towards a synthetic Schlieren method without a reference image, making it possible to use these methods in experiments where taking the reference image is difficult or impossible.

Biblography

o   Aureli F, Dazzi S, Maranzoni A, Mignosa P (2014) A combined colour-infrared imaging technique for measuring water surface over non-horizontal bottom. Experiments in fluids 55(3):1–14

o   Ciddor PE (1996) Refractive index of air: new equations for the visible and near infrared. Applied optics 35(9):1566–1573

o   Daimon M, Masumura A (2007) Measurement of the refractive index of distilled water from the near-infrared region to the ultraviolet region. Applied optics 46(18):3811–3820

o   Dalziel S, Hughes GO, Sutherland BR (2000) Whole-field density measurements by 'synthetic schlieren'. Experiments in Fluids 28(4):322–335

o   Fenton J (1972) A ninth-order solution for the solitary wave. Journal of fluid mechanics 53(02):257–271

o   Gomit G, Chatellier L, Calluaud D, David L (2013) Free surface measurement by stereo-refraction. Experiments in fluids 54(6):1–11

o   Jähne B (1990) Two-dimensional wave nulllber spectra of small-scale water surface waves. Journal of Geophysical Research 95(C7):11–531

o   Jähne B, Schmidt M, Rocholz R (2005) Combined optical slope/height measurements of short wind waves: principle and calibration. Measurement Science and Technology 16(10):1937

o   Kolaas J (2016) Getting started with HydrolabPIV v1.0. Preprint series Research Report in Mechanics

o   Meier G (2002) Computerized background-oriented schlieren. Experiments in Fluids 33(1):181–187

o   Moisy F, Rabaud M, Salsac K (2009) A synthetic schlieren method for the measurement of the topography of a liquid interface. Experiments in Fluids 46(6):1021–1036

o   Russell JS (1844) Report on waves. In: 14th meeting of the British Association for the Advancement of Science, John Murray, London, vol 311, p 390

o   Sellmeier W (1871) Zur erklärung der abnormen farbenfolge im spectrum einiger substanzen. Annalen der Physik und Chemie 219(6):272–282

o   Sultanova N, Kasarova S, Nikolov I (2009) Dispersion proper ties of optical polymers. Acta Physica Polonica-Series A General Physics 19(4):585

o   Sutherland BR, Dalziel SB, Hughes GO, Linden P (1999) Visualization and measurement of internal waves by 'synthetic schlieren'. part 1. Vertically oscillating cylinder. Journal of fluid mechanics 390:93–126

o   Tanaka M (1986) The stability of solitary waves. Physics of Fluids (1958-1988) 29(3):650–655

Acknowledgement